Food & Function

ROYAL SOCIETY OF CHEMISTRY

PAPER

View Article Online
View Journal | View Issue

Cite this: *Food Funct.*, 2021, **12**, 252

Effects of *Pinus massoniana* pollen polysaccharides on intestinal microenvironment and colitis in mice†

Xiangyun Niu, ‡[a,b] Hongqi Shang,‡[a,b] Siyan Chen,[a,b] Ruichang Chen,[a,b] Jin Huang,[a,b] Yongqiang Miao,[a,b] Wenping Cui,[a,b] Huan Wang,[a,b] Zhou Sha,[a,b] Duo Peng*[c] and Ruiliang Zhu*[a,b]

The stability of the intestinal microenvironment is the basis for maintaining the normal physiological activities of the intestine. On the contrary, disordered dynamic processes lead to chronic inflammation and disease pathology. *Pinus massoniana* pollen polysaccharide (PPPS), isolated from *Taishan Pinus massoniana* pollen, has been reported with extensive biological activities, including immune regulation. However, the role of PPPS in the intestinal microenvironment and intestinal diseases is still unknown. In this work, we initiated our investigation by using 16S rRNA high-throughput sequencing technology to assess the effect of PPPS on gut microbiota in mice. The result showed that PPPS regulated the composition of gut microbiota in mice and increased the proportion of probiotics. Subsequently, we established immunosuppressive mice using cyclophosphamide (CTX) and found that PPPS regulated the immunosuppressive state of lymphocytes in Peyer's patches (PPs). Moreover, PPPS also regulated systemic immunity by acting on intestinal PPs. PPPS alleviated lipopolysaccharide (LPS) -induced Caco2 cell damage, indicating that PPPS has the ability to reduce the damage and effectively improve the barrier dysfunction in Caco2 cells. In addition, PPPS alleviated colonic injury and relieved colitis symptoms in dextran sodium sulfate (DSS)-induced colitis mice. Overall, our findings indicate that PPPS shows a practical regulatory effect in the intestinal microenvironment, which provides an essential theoretical basis for us to develop the potential application value of PPPS further.

Received 19th August 2020,
Accepted 6th November 2020

DOI: 10.1039/d0fo02190c

rsc.li/food-function

1. Introduction

The gut is one of the largest organs in the animal body and also an immune organ. The microenvironment of the intestinal tract is composed of gut microbiota, local mucosal immune systems and intestinal epithelial cells, which synergistically stabilize the intestinal functions and health.[1] Any abnormality breaks the balance and leads to the occurrence of diseases. The adult human intestine is home to a vast number of microorganisms.[2] In the long-term evolution process, intestinal microbiota continually interacts with the host to regulate intestinal homeostasis, participate in the metabolism of nutrients in the intestinal tract, and promote the growth and differentiation of intestinal epithelial cells, which resists the invasion and reproduction of external harmful microorganisms,[3] and regulates the intestinal immune function.[4] Intestinal mucosal immunity is the essential component of the mucosal immune system, and the immune cells in the mucosal tissue account for 80% of all the immune cells.[5] Peyer's patches (PPs) are mucous follicular tissues throughout the small intestine of humans and mice. At the terminal ileum, PPs are most evident, which is the primary immune response site exposed to food antigens, pathogens, and vaccines in the gut.[6] The intestinal epithelial barrier in the intestine is the first point of contact with these substances, which is the structural basis of the intestinal mucosal barrier and composed of a mucous layer covering the surface of the intestinal epithelial cell (IEC) with tight junction (TJ). The intestinal epithelial barrier is a selective barrier that allows nutrients, salt, and water from the lumen to enter the bloodstream,[7] and also a protective barrier that prevents intracellular antigens, microorganisms, and toxins from entering the body.[8] Breakdown of the intestinal

[a]*Shandong Provincial Key Laboratory of Animal Biotechnology and Disease Control and Prevention, Shandong Agricultural University, Tai'an, China. E-mail: zhurl@sdau.edu.cn*
[b]*Shandong Provincial Engineering Technology Research Center of Animal Disease Control and Prevention, Shandong Agricultural University, Tai'an, China*
[c]*Department of Immunology and Infectious Diseases, Harvard T.H. Chan School of Public Health, Boston, MA 02115, USA. E-mail: dpeng@hsph.harvard.edu*
†Electronic supplementary information (ESI) available. See DOI: 10.1039/d0fo02190c
‡The co-first author.

microenvironment, especially immune regulatory networks in the intestine, can lead to chronic inflammatory diseases, such as inflammatory bowel disease (IBD).[9] IBD is a chronic, non-specific inflammatory bowel disease of uncertain etiology, including Crohn's disease (CD) and ulcerative colitis (UC). UC mainly affects the colonic mucosa and submucosa, with a gradually increasing incidence rate, especially in adults and children in recent years.[10] the current therapeutic approaches for IBD include control of inflammatory responses and regulation of immune disorders, which only reduce symptoms or suppress exacerbations. On the other hand, available treatments for severe cases are limited without an effective cure.[11] Therefore, the discovery of a safe and effective drug for patients with UC is crucial.

Polysaccharides are polymerized carbohydrate macromolecules formed by long-chain monosaccharide units connected by glycoside linkages.[12] Plant polysaccharides have a long history of being considered as a kind of living and energy substance. While a number of studies have revealed that they have various pharmacological effects, including immune regulation,[13] anti-oxidant,[14]anti-tumor,[14] anti-virus,[15] hypoglycemic[16] and so on.[17] Some polysaccharides (*e.g.* Astragalus polysaccharides) have been developed as commercial immunostimulants and adjuvants for the control of animal diseases. Pine pollen, known as the "king of pollen" in China, is nutritional pollen with a variety of biological activities. Previous efforts in our laboratory have led to the identification of *Taishan Pinus massoniana* pollen polysaccharides (PPPS) that exhibited good antioxidant, immunoregulatory, and anti-viral activities.[18] However, it is still unclear that if PPPS is able to interact with intestinal microenvironment and have effects on gut-related diseases.

In this study, our results showed that PPPS regulated gut microbiota and increased the proportion of probiotics in the intestinal tract in mice. In a CTX-induced immunosuppressive mouse model, PPPS maintained the portion of B and T cells and their subsets in PPs while raising the secretion of sIgA in the intestine to normal levels under immunosuppression. We also found that PPPS regulated systemic immunity through PPs. We demonstrated that PPPS mitigated lipopolysaccharide (LPS)-induced intestinal epithelial damage in Caco2 monolayer cells. In the end, orally administrated PPPS significantly alleviated the colitis injury in dextran sodium sulfate (DSS)-induced colitis mice. Therefore, PPPS has the ability to maintain the homeostasis of the intestinal microenvironment, which is a promising strategy in treating inflammatory intestinal diseases.

2. Materials & methods

2.1 Preparation of polysaccharide

PPPS was extracted from the pollen of the *Taishan pinus massoniana* based on a previously established protocol.[18] The purity of the obtained PPPS was analyzed by phonel-sulfate method and was shown to be 90.6%.

2.2 Microbiota 16S rRNA gene sequencing

BALB/c mice were administered by PPPS (150 mg kg^{-1}) or equal volume phosphate buffered saline (PBS) gavage for two weeks (n = 3 mice). Bacterial DNA from fecal samples were isolated with CTAB method. The purity of DNA were determined by agarose gel electrophoresis. Bacterial strains were investigated using 16S rRNA gene sequencing. DNA was used as a template to amplify using a Phusion® High-Fidelity PCR Master Mix (New England Biolabs, USA). The v4 regions of 16S ribosomal RNA gene were amplified using specific primers with Barcode 515F (5′-GTGCCAGCMGCCGCGGTAA-3′) and 806R (5′-GGACTACHVGGGTWTCTAAT-3′). PCR products were detected by electrophoresis with 2% agarose gel and recovered by GeneJET PCR Kit (Thermo Scientific, USA). Ion Plus Fragment Library Kit 48 RXNS construction Kit (Thermo Scientific) was used for Library construction, Ion S5TMXL Sequencing platform (Thermo Scientific, USA) was used for sequencing. By applying Uparse software (Uparse v7.0.1001, http://www.drive5.com/uparse/) the species clustering was determined based on the operational taxonomic unit (OTU) using amplicon sequencing of 16S RNA. The reference sequences allowed sorting of the results into OTUs by clustering 97% sequence similarity. The microbial classification was performed with Mothur method and SILVA132 (http://www.arb-silva.de/) SSUrRNA database and classification according to various taxonomic ranks (phylum, order, class, family, genus, and species). The alpha diversity index was analyzed using QIIME software (Version 1.9.1, http://www.qiime.org) and percentage of each bacterial species was virtualized with R software (Version 2.15.3).

2.3 Quantitative of gut bacteria using qPCR

For gut bacteria identification, qPCR was performed from fecal samples isolated with CTAB method. Quantitation was performed using ChamQ Universal SYBR qPCR Master Mix (vazyme, China) according to the user manufacturer's instructions, and the bacterial specific primers are listed in Table 1. qPCR was performed using ABI 7500 Real-Time PCR system (Applied Biosystems, USA) with each reaction run in triplicate. Analysis and fold-change were determined using the comparative threshold cycle (Ct) method.

2.4 Experimental animals and immunosuppressive model

The BALB/c female mice were provided by Shandong Laboratory Animal Center and adapted in Specific Pathogen Free (SPF) level environment. Thirty 6-week-old mice at 6 weeks of age were housed based on their genotypes and used. During the experiment, animals were raised with constant temperature (21–23 °C) and constant humidity (50–60%), 12 h of light and 12 h of darkness, and free intake of drinking water and feed. Seven days after oral administration of PPPS in the experimental group and equal volume of PBS in the control group, mice (n = 6 mice) were injected with CTX (CAS# 6055-19-2, Aladdin, China) intraperitoneally and used at a dose of 100 mg kg^{-1}. And we set up three different concentrations of PPPS, PPPS low dosage (PPPSL, 50 mg/kg/day),

Table 1 Bacteria primer sequence for qPCR

Name	Forward (5′–3′)	Reverse (5′–3′)
Lactobacillaceae	CGCATAACAACTTGGACCGCATGG	CTCAGGTCGGCTACGTATCATTGC
Bacteroidaceae	CGATGATACGCGAGGAACCTTACC	CGGCACGAGCTGACGACAAC
Muribaculaceae	GCTGCCTAAGCGGAACCTCTAAC	CCTTCGCCATCGGTGTTCTTCC
Xanthobacteraceae	CTAGCGTTGCTCGGAATCACTGG	CGCCTTCGCCACTGGTGTTC
Rikenellaceae	GATGCGGTAGGCGGAATGTATGG	TGGTAAGCTGCCTTCGCAATCG
Prevotellaceae	TGGTCAATGGACGCAAGTCTGAAC	CGGCTGCTGGCACGGAATTAG
Sphingomonadaceae	GCATCGCTTGAATCCAGGAGAGG	CCTTCGCCACTGGTGTTCTTCC
Bifidobacteriaceae	TCGAATAAGCACCGGCTAACTACG	GGCGCGGATCCACCGTTAAG
Paenibacillaceae	TCTTCCGCAATGGACGCAAGTC	CGGCTGCTGGCACGTAGTTAG
Lachnospiraceae	AGCTGGAGTGCAGGAGAGGTAAG	CGCCTTCGCCACTGGTGTTC
16S Universal	CCTACGGGAGGCAGCAG	ATTACCGCGGCTGCTGG

PPPS moderate dosage (PPPSM, 125 mg/kg/day) and PPPS high dosage (PPPSH, 250 mg/kg/day) for the experiment. The flow cytometry analysis and ELISA test was performed 24 hours later, and the operation process of the experiment will be briefly described below. The animal experiments were approved by Animal Protection and Utilization Committee of Shandong Agricultural University (Permit number: 20010510) and executed in accordance with Guide to Animal Experiments of Ministry of Science and Technology (Beijing, China). This study did not involve any endangered or protected species.

2.5 Enzyme-linked immunosorbent assay (ELISA)

The cytokine IL-6 and GM-CSF levels in cell culture supernatants and the sIgA in mouse colon mucus were quantified using ELISA kits (Lengton, China) according to the manufacturer's instructions. The absorbance (OD value) of each hole was measured by SpectraMax i3x (Molecular Devices, USA) in sequence at the wavelength of 450 nm and zero of blank air conditioner.

2.6 Isolation of lymphocytes and flow cytometry

The isolation of lymphocytes was performed as previously described.[19] The mice were euthanized by carbon dioxide asphyxiation. Before surgery, 75% ethanol was used to cleansed the abdomen of the mice, the abdominal cavity was opened, and the small intestine of the mice was completely separated. Lay the small intestine flat on a soaked gauze, and the individual lymph nodes can be clearly seen on the anti-mesenteric side of the intestine. The entire PPs was separated with scissors and placed into cold Hank's Balanced Salt Solution (HBSS). In order to obtain the single-cell suspension, lymph nodes were transferred to a 70-micron size sieve, and the piston base of a 1 ml syringe was used to press the lymph nodes to grind the tissue. Finally, the sieve was rinsed and cell suspension was collected. EDTA was added to make the final concentration 1 mM. The cell suspension was centrifuged (5 min, 450*g*), and the cells were resuspended with flow buffer (phosphate buffered saline containing 1% fetal calf serum). Cells were stained with 0.1% trypan blue (TBD, China), the number of cells was counted, and the cell concentration was adjusted to 1×10^6/cells in 100 μl. FACS antibodies include: APC anti-mouse CD3 (BioLegend, USA), FITC anti-mouse CD4 (BioLegend, USA), PE anti-mouse CD8 (BioLegend, USA), PerCP/Cyanine5.5 anti-mouse CD19 (BioLegend, USA). Single cell suspensions were labeled with antibodies in flow buffer for 30 min on ice. Data were acquired using a BD LSRFortessa 4 flow cytometer (BD Biosciences, San Jose, CA) and analyzed using FlowJo software (Tree Star Inc., Ashland, OR).

2.7 Intestinal immune system modulating activity assay

Intestinal immune system modulating activity through Peyer's patch was measured according to the previously described.[20] Briefly, suspensions of Peyer's patch cells in RPMI 1640 medium (Solarbio, China) supplemented with 5% FBS (RPMl 1640-FBS) were prepared from a small intestine of BALB/c mice (6 weeks old). 200 μl cell suspension (2×10^6 cells per ml in RPMI 1640-FBS) were cultured with test sample in 96 well flat bottom plate for 5 days at 37 °C in a humidified atmosphere of 5% CO_2–95% air. The resulting culture supernatant (50 μL) was incubated with bone marrow cells suspension (2×10^5 cells per ml) from BALB/c mice for 6 days in a humidified atmosphere of 5% CO_2–95% air. After 20μl of Alamar Blue™ solution (Maokang Biotechnology, China) was added to each well, the cells were then continuously cultured for 5–24 h. The fluorescence intensity was measured to count cell numbers by SpectraMax i3x (Molecular Devices, USA) at an excitation wavelength of 544 nm and emission wavelength of 590 nm during cultivation.

2.8 Cell culture

Caco2 cells were grown in a culture medium composed of minimum Eagle's medium (MEM) medium (Solarbio, China), 100 U ml^{-1} penicillin,0.1 mg ml^{-1} streptomycin, and 10% (v/v) heat-inactivated FBS in 25 cm^2 tissue culture flasks (Beaver, China). The cells were maintained at 37 °C in an atmosphere of 5% CO_2/95% air incubator.

2.9 Cell viability

Cell viability was measured by Cell Counting Kit-8 (MCE, USA) according to the manufacturer's instructions. Caco2 cells were plated in 96-well culture plates at a density of 6000 cells per well before treatment. Caco2 cells were treated or not treated with PPPS 3, 6, 12 and 24 h prior to addition of 100 μg ml^{-1} LPS and the cell viability was measured at 24 h, 10 μL of the CCK-8

solution was added to each filter, and reaction was allowed to occur under standard culture conditions for 1 h. Absorbance was measured at 450 nm using a SpectraMax i3x (Molecular Devices, USA).

2.10 Transepithelial electrical resistance (TER)

Caco2 cells were seed at 10^5 cells per mL in the 0.33 and 1.12cm^2 transwells insert (Costar, Corning, USA) with 0.4 μm sizes pore. Medium should be changed on days 4, 8, 12, 16 and 18 until complete differentiation had taken place. Caco2 cells were treated or not treated with PPPS 3 h prior to addition of 100 μg ml^{-1} LPS and the transepithelial electrical resistance (TER) was measured at 3 h. The electrical resistance was measured using the Millicell-ERS electrical resistance system (Millipore, Bedford, MA). During measurement, both apical and basolateral sides of the epithelium were bathed with buffer solution. Electrical resistance was measured until similar values were recorded for three consecutive measurements. TER values were expressed as Ω cm^2.

2.11 Epithelial paracellular permeability

Paracellular permeability was determined using the nonabsorbable FITC-conjugated dextran probe (CAS# 60842-46-8, MW: 3000–5000, Aladdin, China). Caco2 cells were seeded in 0.33 cm^2 Transwell chamber with 0.4 mm pores. Caco2 cells were treated or not treated with PPPS 3 h prior to addition of 100 μg ml^{-1} LPS. Before experimental treatment, the apical and basolateral compartments were washed with sterile PBS. Then PBS was added to the apical and basolateral compartment, and the FITC-dextran (10 mg ml^{-1}) was added to the apical compartment with 5 μL. After 1 h incubation at 37 °C, 100 μL buffer from the basolateral compartment was added to a 96-well plate, and the absorbance was determined by using a SpectraMax i3x (Molecular Devices, USA). The excitation and emission wavelengths were 490 and 520 nm, respectively.

2.12 Western blot

1×10^5 Caco2 cells per well were seeded in 6-well tissue culture and treated or not treated with PPPS 3 h prior to addition of 100 μg ml^{-1} LPS. At the end of the experiment, Caco2 monolayers were immediately washed with ice-cold PBS, and cells were lysed with radio-immunoprecipitation assay (RIPA) lysis buffer (Beyotime, China) with the addition of protease and phosphatase inhibitors for 5 min. Cell lysates were centrifuged at 14 000*g* for 30 min. The supernatant was collected, and protein was measured using the BCA Protein Assay Kit (Beyotime, China). SDS-PAGE Sample Loading Buffer (5−; Beyotime, China) was added to the lysate containing 20–30 μg of protein and boiled for 10 min, after which equal amounts of protein for each sample was separated on 10% SDS-PAGE gel. Proteins from the gel were transferred to nitrocellulose membrane (Millipore, USA). The membranes were blocked in 5% non-fat milk in TBS containing 0.05% Tween-20 (TBST) buffer for 1 h, and then incubated with appropriate primary antibodies anti-ZO-1 (Proteintech, China) at 1 : 1000, anti-Occludin (Proteintech, China) at 1 : 2000 and anti-GAPDH (Beyotime, China) at 1 : 2000 overnight at 4 °C. After being washed in TBS-T buffer, the membranes were incubated with appropriate secondary antibodies for 1 h at room temperature. Signal was detected with an ECL kit (Beyotime, China) and western blot densitometry analysis was performed using Image-J software (http://rsbweb.nih.gov/ij/). The band density was normalized to the endogenous reference GAPDH.

2.13 Mouse model with DSS-induced colitis

Colitis was induced by addition of dextran sulfate sodium (DSS, MW 36 000–50 000, Aladdin, China) to autoclaved drinking water at 3% (w/v) for 7 days (n = 5 mice). The DSS solutions were made freshly every three days. Similarly, we set up three different concentrations of PPPS, PPPS low dosage (PPPSL, 50 mg/kg/day), PPPS moderate dosage (PPPSM, 125 mg/kg/day) and PPPS high dosage (PPPSH, 250 mg/kg/day). The development of colitis was monitored by measuring the mice's daily weight and blood in the stool. Stool consistency and rectal bleeding were scored according to a previously described protocol.[21] Briefly, stool scores were determined as: 0 = normal stool, 1 = soft stool but still formed, 2 = very soft stool, 3 = diarrhea. Bleeding scores were determined as: 0 = no bleed, 1 = positive hemoccult, 2 = visible blood in stool, 3 = gross rectal bleeding. Stool scores and bleeding scores were added as clinical score.

2.14 Histological analysis

For hematoxylin and eosin (H&E) staining, the colon tissue was fixed overnight with 4% formalin buffer at 4 °C, then soaked in 70%, 80%, 95% and 100% graded ethanol for 40 minutes, dehydrated, and transparent with xylene. The slices were then cut into ultrathin slices (5 μm) with a slicer, baked in a 60 °C incubator for 1 hour, dewaxed in xylene, hydrated and stained with H&E, and sealed with neutral resin. Histologic change scores was performed as previously described.[21] Briefly, histological scores were determined as: 0 = no evidence of inflammation, 1 = low level of inflammation with scattered infiltrating mononuclear cells (1–2 foci), 2 = moderate inflammation with multiple foci, 3 = high level of inflammation with increased vascular density and marked wall thickening, 4 = maximal severity of inflammation with transmural leukocyte infiltration and loss of goblet cells.

2.15 Quantitative real-time PCR for RNA expression

Total RNA of colon tissue isolated by using the TRIzol reagent (CWBIO, China). cDNA was synthesized with HiScript IIQ RT SuperMix (Vazyme, China) according to the manufacturer's instructions. qRT-PCR was performed with ChamQ Universal SYBR qPCR Master Mix (Vazyme, China) in ABI 7500 Real-Time PCR system (Applied Biosystems, USA). Relative mRNA levels were normalized to the endogenous control gene GAPDH. qPCR system with each reaction run in triplicate. Analysis and relative expression were determined using the comparative threshold cycle (Ct) method. Primers used in this paper were listed in Table 2.

Table 2 Mouse primer sequence for qRT-PCR

Name	Forward (5′–3′)	Reverse (5′–3′)
TNF-α	CTGGCCTCTCTACCTTGTTGC	CTGGCCTCTCTACCTTGTTGC
IL-1β	TCTGAAGCAGCTATGGCAAC	TTCATCTTTTGGGGTCCGTCA
IL-6	AGTCAATTCCAGAAACCGCTA	GTCACCAGCATCAGTCCCAA
IL-10	ACCTGCCTAACATGCTTCGAG	TTGGCAACCCAGGTAACCCTT
IL-4	TGAGCTCGTCTGTAGGGCTT	CTGCAGCTCCATGAGAACACT
IL-22	CCTATATCACCAACCGCACCT	CGCTCACTCATACTGACTCCG
GAPDH	GGTTGTCTCCTGCGACTTCA	TGGTCCAGGGTTTCTTACTCC

2.16 Bacterial translocation

The transfer of bacteria from the intestinal tract to the peripheral blood and liver is indicated by the number of *Lactobacillus* and *Escherichia coli* (*E. coli*). Among them, *Lactobacillus* is used as probiotic indicator bacteria, and *E. coli* is as indicator bacteria of harmful bacteria. 50 μl of anticoagulant blood were cultured on MRS and EMB agar for 36 h at 37 °C. Liver tissue samples were homogenized in 0.5% Triton X-100/PBS, and 100 μL of the homogenates were cultured on MRS and EMB agar plates similarly. After 36 h of incubation, CFUs were counted, and the results are expressed as number of bacteria detected per mL of blood or gram of liver.

2.17 Statistics

All statistical analyses in this study were performed with SPSS 17.0 software. The data are presented as values with standard deviation (as the mean ± SD). Differences between individual groups were analyzed *via* one- or two-way ANOVA. *P* values were indicated and $P < 0.05$ was considered significant. $^{*}P < 0.05$; $^{**}P < 0.01$; $^{***}P < 0.001$; ns, not significant. "*n*" indicates biological replicates for *in vitro* experiments and number of mice for *in vivo* studies. Animals subjects were randomly assigned to a control group and different experimental condition groups matched for age and sex using simple randomization.

3. Results

3.1 PPPS can affect the composition of gut microbiota in mice

To explore the effect of PPPS on the gut microbiota of mice, we used 16S rRNA sequencing to analyze the gut microbiota changes in mice. The dilution curve showed a definite turning point when the sequencing volume was around 30 000, followed by an extended period, which indicates that the sequencing depth was sufficient (Fig. 1A). Alpha diversity analysis showed that PPPS-treated mice had more abundant gut microbiota than that of the PBS group mice (Fig. 1B). The histogram of the intestinal microbial community structure revealed the microbial species and their relative abundance. At the phylum level, compared with PBS group, *Firmicutes*, *Bacteroidetes*, *Proteobacteria*, *Actinobacteria*, *Cyanobacteria*, *Melainabacteria*, and *Armatimonadetes* had higher relative abundance in PPPS group mice relative to the PBS group. In comparison, the relative abundance of *Tenericutes* and *Deferribacteres* was lower (Fig. 1C). At the family level, the relative abundance of *Bacteroidaceae*, *Muribaculaceae*, *Xanthobacteraceae*, *Rikenellaceae*, *Prevoteliaceae*, *Sphingobacteriaceae*, *Bifidobacteriaceae*, and *Paenibacillaceae* in the PPPS group was higher than that in the PBS group. In contrast, *Lactobacillaceae* and *Lachnospiraceae* were less (Fig. 1D). qPCR assay was performed to verify the results of the sequencing analysis at the level of the family. We found that there was a significant increase in the relative abundance of *Bacteroidaceae*, *Muribaculaceae*, *Rikenellaceae*, *Prevoteliaceae*, *Bifidobacteriaceae*, and *Lachnospiraceae* after treating with PPPS, which is consistent with the 16S rRNA sequencing results (Fig. 1E). These findings indicate that PPPS can increase the proportion and diversity of gut beneficial bacteria in mice, which plays a decisive role in slowing down metabolic disorders and resisting inflammatory factors.

3.2 PPPS activates the immune response of PPs lymphocytes in CTX-induced immunosuppressive mice

To investigate the effect of PPPS in intestinal mucosal immunity, especially in PPs, we generated immunosuppressed mice with CTX injections. The results showed that CTX injections reduced the secretion of sIgA (Fig. 2G) and proportion of B cells (Fig. 2I) and $CD3^{+}CD4^{+}$T cells (Fig. 2D) in intestinal. Firstly, the gavage administration of PPPS did not affect the weight of mice and the size of Peyer's patches as compared to the PBS group mice (data not shown). The intestinal sIgA secretion and lymphocyte percentage in PPs were measured in immunosuppression mice. Lymphocytes in PPs were isolated, and the B, T cells and their subsets were analyzed by flow cytometry. In the immunosuppression mice, PPPS significantly increased the proportion of $CD3^{+}$T cells (Fig. 2A and B) and restored the reduced percentage of $CD3^{+}CD4^{+}$T cell subsets caused by CTX (Fig. 2C and D) while maintaining the ratio of $CD3^{+}CD4^{+}/CD3^{+}CD8^{+}$T cell subsets (Fig. 2F). At the same time, there was no statistically significant difference in $CD3^{+}CD8^{+}$T cells (Fig. 2E). The ELISA results showed that PPPS significantly relieved the decrease of sIgA (Fig. 2G). PPPS significantly increased the proportion of B cells (Fig. 2H and I). These results suggest that PPPS has an activation effect on the intestinal mucosal immune system and activates the immune response to PPs lymphocytes under immunosuppressed conditions.

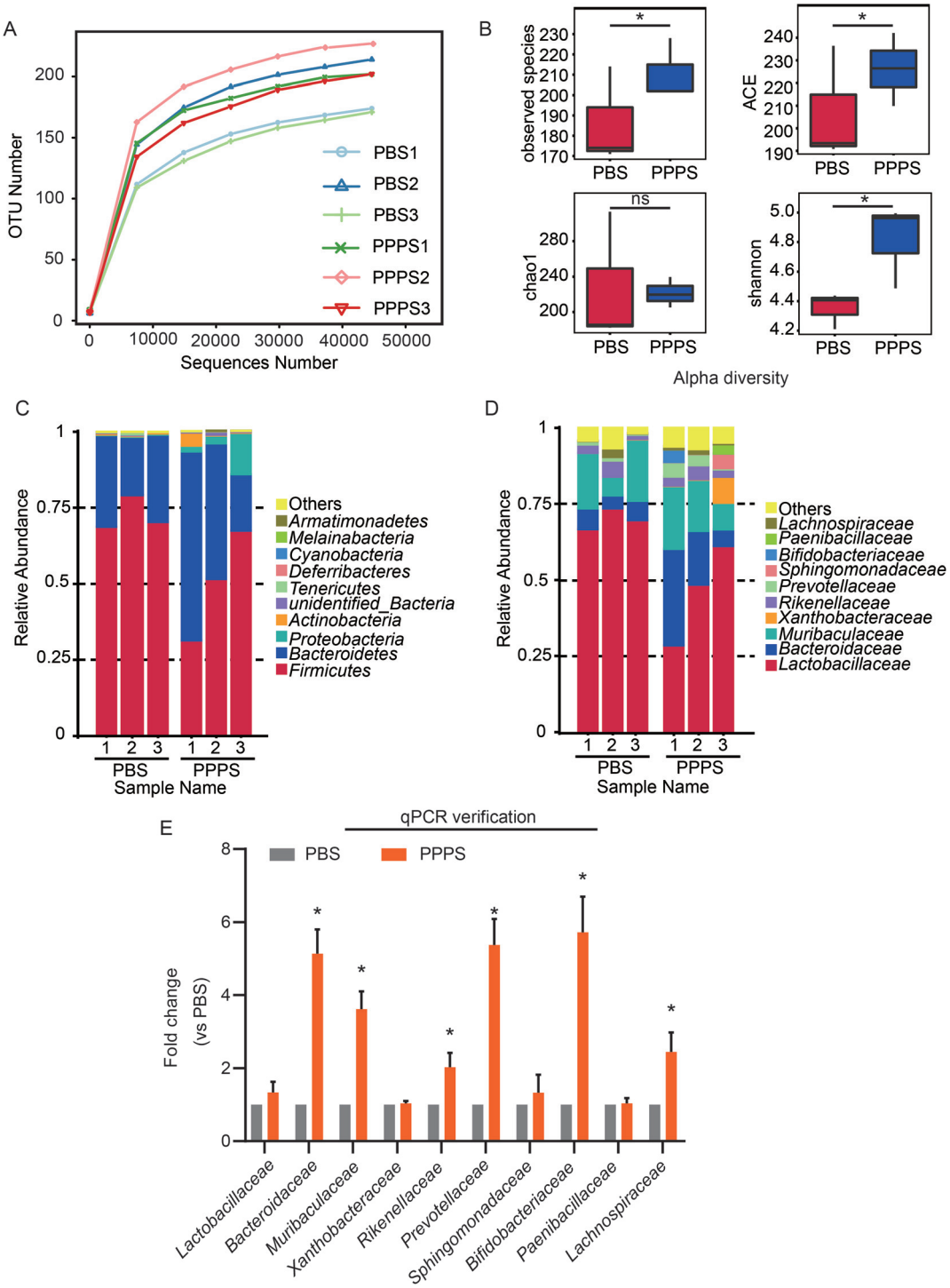

Fig. 1 PPPS affects gut microbiota composition in mice. Mice were fed with PPPS for 7 days, 125 mg kg^{-1} each time, in the control group were fed with PBS of the same volume. At day 15, bacterial DNA from feces was evaluated using 16S rRNA gene sequencing (n = 3 mice). (A) Observation of species dilution curve of bacteria in mice feces. (B) Alpha diversity index of bacteria, include observed species, ACE, Chao 1, Shannon. The relative abundance distribution shows the percentage of top 10 bacteria sequence in all sequence reads at the level of phylum (C) and family (D). Others represent taxa beyond the top 10 taxa in phylum and family levels. (E) At the level of family reads, top 10 bacteria identified by qPCR in feces of mice, qPCR reaction is performed three times. PBS1, PBS2, PBS3 represent three repeated PBS groups; PPPS1, PPPS2, PPPS3 represent three repeated PPPS groups respectively. PPPS *versus* PBS. *p < 0.05 and **p < 0.01 (two-tailed t test); ns, not significant.

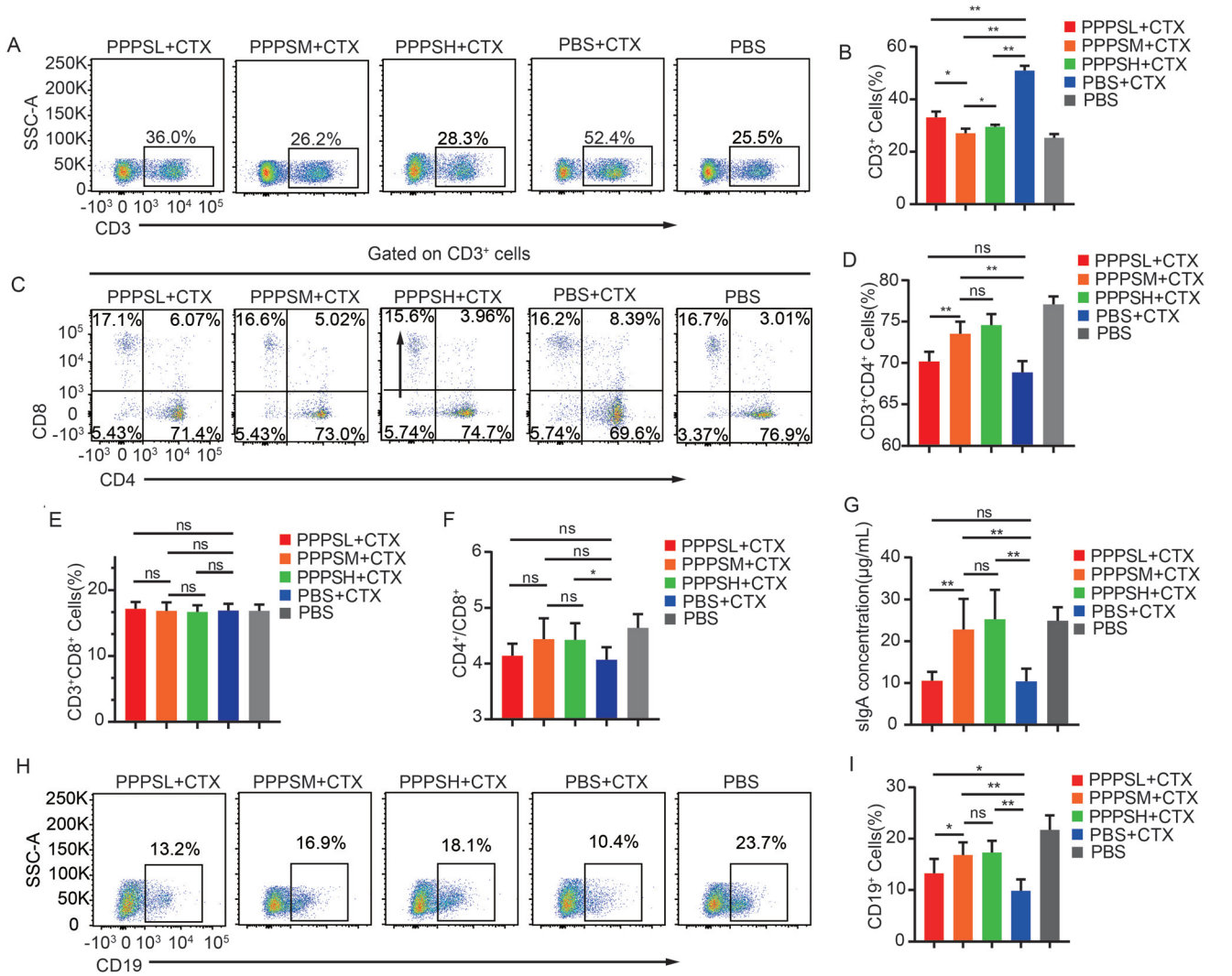

Fig. 2 PPPS affects the immune status of lymphocytes in PPs. (A) Changes in the secretion of sIgA in the small intestinal lumen of mice. (B and C) Flow cytometry was used to detect $CD19^+$ cells for analyzing the changes (B) and percentages (C) of B cells in the PPs. (D–E) $CD3^+$ cells for analyzing the changes (D) and percentages (E) of T cells in the PPs. (F–H) $CD3^+$ $CD4^+$ and $CD3^+$ $CD8^+$ cells for analyzing the changes (F) and percentages (G and H) of T cells subsets in the PPs.(I) The ratio of $CD3^+CD4^+$T cells to $CD4^+CD8^+$T cells subsets in PPs. The data (A, B, D and F) are representative of three independent experiments (error bars, SD). PPPSL, PPPS low dosage (50 mg mL^{-1}); PPPSM, PPPS moderate dosage (125 mg mL^{-1}); PPPSH, PPPS high dosage (250 mg mL^{-1}). *$p < 0.05$ and **$p < 0.01$ (two-tailed t test); ns, not significant.

3.3 PPPS have PP-mediated intestinal immune system modulating activity

The effects of the PPPS on PP-mediated intestinal immune system modulation were investigated in mice. In *ex vivo* experiment, when the mice were orally given PPPS for 14 days, a significant increase in activity of bone marrow cells was observed on the 5th day and activity was maintained until the 14st day (Fig. 3A). These results indicate that PPPS is a potent inducer of hematopoietic growth factor. In order to know whether PPPS induces granulocyte-macrophage colony stimulating factor (GM-CSF) and/or Interleukin-6 (IL-6) secretion from PPs cells, PPs cells from mice were cultured and treated with cultivated with PPPS for 5 days *in vitro*. The ELISA results showed that PPPS could significantly increase the secretion of GM-CSF and IL-6 in cell culture supernatant in comparison with the PBS group (Fig. 3B and C), and Alamar Blue™ test results showed that supernatant of lymphocytes treated with PPPS showed the significantly promoted proliferation of mouse bone marrow cells (Fig. 3D). This study results demonstrate that PPPS can modulate intestinal immune activity through the PP-mediated mucosal immunity but also the systemic immune system through PPs.

3.4 PPPS attenuated LPS-induced epithelial barrier damage

Furthermore, we initially examined the effect of PPPS on the viability of human colon epithelial Caco2 cells to explore the role of PPPS in the intestinal epithelial barrier. The results showed that PPPS did not affect the viability of Caco2 cells under no stress (Fig. 4A). Therefore, we used LPS to induce Caco2 cell barrier damage, and then examined the changes in

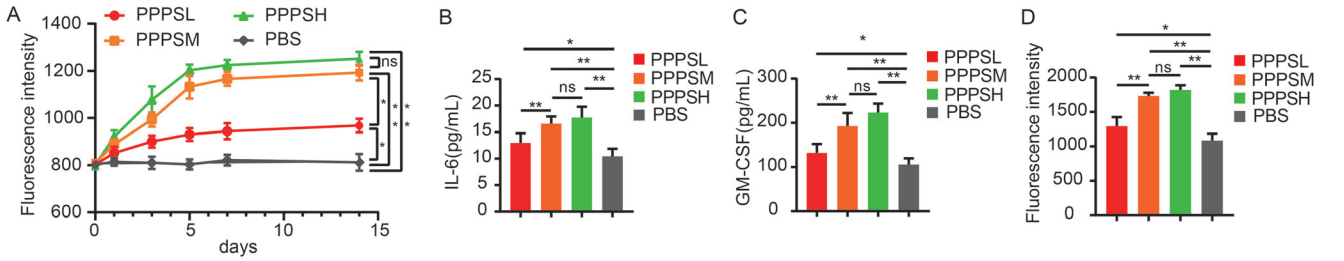

Fig. 3 PPPS could modulates the intestinal immune system through Peyer's patches. Lymphocyte cells in PPs of mice were cultured *in vitro* and stimulated by PPPS (n = 5). Change of proliferation activity of bone marrow cells for 14 consecutive days (A). The secretion of GM-CSF and IL-6 was detected (B and C). The supernatant after PPPS treatment was added to the cultured mouse bone marrow cells *in vitro* to detect the proliferation of bone marrow cells (D). The data (A–D) are representative of three independent experiments (error bars, SD). PPPSL, PPPS low dosage (100 μg mL^{-1}); PPPSM, PPPS moderate dosage (200 μg mL^{-1}); PPPSH, PPPS high dosage (400 μg mL^{-1}). *p < 0.05 and **p < 0.01 (two-tailed t test); ns, not significant.

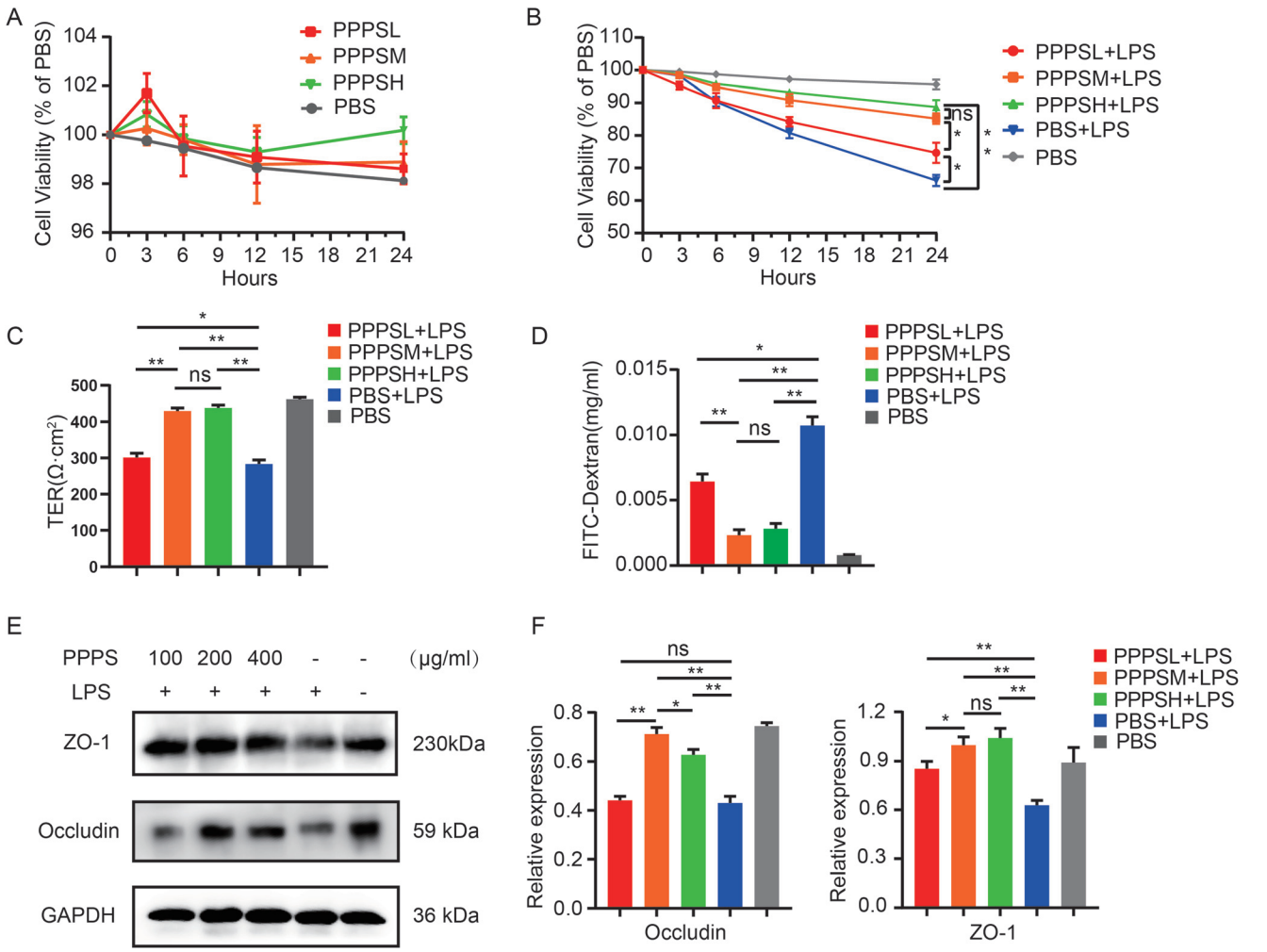

Fig. 4 Effect of PPPS pretreatment on mucosal barrier function in Caco2 cells under LPS stimulation. (A) The activity of Caco2 cells was detected by cck-8 after PPPS stimulation. (B) Changes of cell activity after different pretreatment time with PPPS (C and D) Caco2 monolayer cells were pretreated with different concentrations PPPS 3 h prior to LPS and co-cultured for 24 h, the transepithelial electrical resistance (TER) (C) and FITC-dextran permeability (D) of Caco2 monolayer cells were measured. (E and F) The western blotting detected changes in occludin and zo-1 expression, values were normalized to GAPDH. The data (A–F) are representative of three independent experiments (error bars, SD). PPPSL, PPPS low dosage (100 μg mL^{-1}); PPPSM, PPPS moderate dosage (200 μg mL^{-1}); PPPSH, PPPS high dosage (400 μg mL^{-1}). *p < 0.05 and **p < 0.01 (two-tailed t test); ns, not significant.

cell viability, barrier integrity, permeability, expression distribution, and levels of tight junction proteins, such as occludin and ZO-1, after PPPS pretreatment. The results showed that PPPS significantly increased the cell viability (Fig. 4B), improved the transepithelial electrical resistance (TER) (Fig. 4C), and reduced the FITC-dextran permeability (Fig. 4D) compared to the PBS group. We further found that the protein levels of occludin and ZO-1 determined by western-blot assay were also higher in PPPS treated Caco2 cells (Fig. 4E and F). These data indicate that PPPS can alleviate the Caco2 cell barrier damage induced by LPS while protecting the function of the intestinal epithelial barrier.

3.5 PPPS protected mice from DSS-induced colitis

Given the positive regulation of PPPS on the intestinal tract microenvironment, a DSS-induced colitis mice model was established to explore the role of PPPS in mouse colitis. It was evident that PPPS partially rescued the weight loss of mice (Fig. 5A) and reduced the clinical scores indicated by diarrhea and rectal bleeding (Fig. 5B). Mice were sacrificed and dissected on day 8, and we found that PPPS significantly increased the length of the colon compared to the group treated with DSS only (Fig. 5C and D). Histological analysis revealed that PPPS reduced mucosal damage and dampened inflammatory responses in the colon, while the groups treated with PPPS had lower histological scores (Fig. 5E and F). Additionally, we examined the mRNA expression of cytokine related to Inflammation response in the colon tissues. The results suggested that the expression levels of TNF-α, IL-1β, and IL-6 were significantly reduced, while the levels of IL-4, IL-10, and IL-22 were significantly increased in the colon of PPPS treated mice compared to those mice only treated with DSS (Fig. 6). Bacterial translocation analysis showed that PPPS reduced the migration of *Lactobacillus* (Fig. S1A† and Fig. 7A) and *E. coli* (Fig. S1B† and Fig. 7B) into the bloodstream and liver in mice compared to the vehicle group. These results demonstrate that PPPS can significantly relieve DSS-induced colitis while retaining intestinal stability in mice.

4. Discussion

Intestinal microbiota, mucosal immunity, and epithelial cells play an important role in maintaining the dynamic balance of the intestine. On the contrary, abnormalities in the aforementioned three factors, and primarily intestinal mucosal immune, are significant causes of the pathogenesis of inflammatory bowel disease (IBD).[22] Many plant polysaccharides possess biological activities including various regulatory functions in the physiological activities of humans and animals. Our previous studies have demonstrated that PPPS, as a new type of plant polysaccharide, has antiviral, including subgroup B/J avian leukosis virus,[23–25] and immunomodulatory properties. However, it is still unknown if PPPS affects intestinal microenvironment and has therapeutic effects on gut-related diseases. Here we report that PPPS can regulate gut microbiota and increase the proportion of probiotics in the intestinal tract in mice. Moreover, PPPS can activate the immune response in the intestine of immunosuppressed mice and also affect the cytokine secretion in PPs. In addition, we have revealed that PPPS can alleviate LPS-induced intestinal epithelial damage and relieve the damage by DSS-induced colitis in mice.

Gut microbiota and organisms depend on each other while constituting the intestinal micro-ecosystem. In a balanced state, the micro-ecosystem can promote the digestion of food (*e.g.*, cellulose), produce a variety of nutrients, and stimulate the immune response of the body to resist the invasion of foreign pathogens.[26,27] In our study, 16S rRNA deep sequencing and 16S qPCR results have demonstrated that PPPS can change the composition of the gut microbiome in mice, including the increased proportion of *Bacteroidaceae*, *Muribaculaceae*, *Rikenellaceae*, *Prevotellaceae*, *Bifidobacteriaceae*, and *Lachnospiracea*. The gut microbiome is dominated by four Phyla: *Firmicutes*, *Bacteroidetes*, *Proteobacteria*, and *Actinobacteria.*[28] Among them, *Bacteroidaceae*, *Muribaculaceae*, *Rikenellaceae*, *Prevotellaceae* belong to *Bacteroidetes*, which help the host decompose complex polysaccharides to improve nutrient acquisition,[29] accelerate the formation of intestinal mucosa vessels,[30] maintain the intestinal microecological balance,[31] and produce the short-chain fatty acids acetate and propionate. All these microbes can be considered as a source of energy, participants of metabolism of substances, and assistants in high fiber and high carbohydrate dietary intake.[32] *Bifidobacteriaceae*, which belongs to *Actinobacteria*, mainly residing in the gastrointestinal tract of the human body, has a variety of physiological effect, including nutritional,[33] bacteriostatic,[34] laxative,[35] anti-aging,[36] cardiovascular disease prevention,[37] immunity and anti-cancer[38] roles. On the other hand, *Lachnospiracea*, which belongs to *Firmicutes*, has the ability to affect the number and function of T_{reg} cells. It has been speculated that *Lachnospiraceae* may regulate the immune balance of T_{reg}/Th17 by regulating the protein expression level in $CD4^+$T cells.[39] In previous studies have shown that the pine pollen can reduce the fecal germ contents of *Proteus mirabilis* and *E. coli*,[40] and PPPS may be the main component in pine pollen that plays a critical role in the effect on gut microbiota. The network regulated by these gut bacteria after PPPS treatment remain unclear, thus requiring further study.

Peyer's patches (PPs) are considered as the leading induction site of the intestinal mucosal immune response in the gut-associated lymphoid tissue (GALT). Targeted delivery of drugs or bioactive substances to PPs benefits the treatment of intestinal immune-related diseases. PPs can be anatomically subdivided into multiple B cell follicles, surrounded by T cell-rich interfollicular regions (IFR), and covered by specialized follicle-associated epithelium (FAE) which specialized cells named microfold (M) cells.[41] Intracellular antigen was directly taken by M cells in PPs and treated by antigen-presenting cells (APC) to sensitize immature T cells and B cells in the circulation.[42] The sensitized T and B lymphocytes can further enter the blood circulation, and ultimately arrive at the laminae

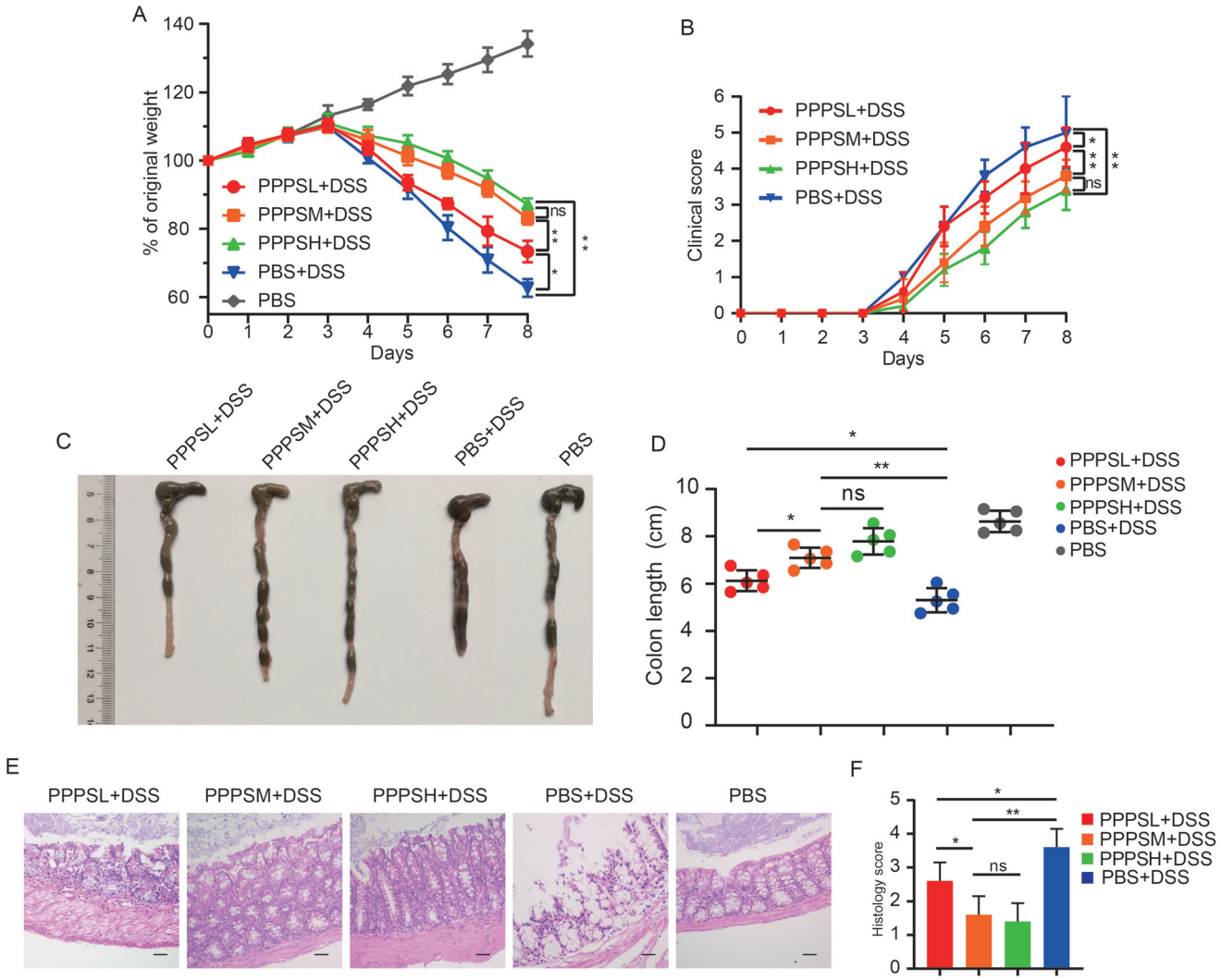

Fig. 5 PPPS can relieve symptoms of colitis DSS-induced in mice. Body weight (A) and clinical score (B) were recorded daily. At day 8, representative colons from mice treated as labeled in the figure (C) and quantification of colon length (D). Representative hematoxylin and eosin staining of colon section (E) and histology score (F) are shown (n = 5) (scale bars: F, 100 μm). The data (A–F) are representative of three independent experiments (error bars, SD). PPPSL, PPPS low dosage (50 mg mL^{-1}); PPPSM, PPPS moderate dosage (125 mg mL^{-1}); PPPSH, PPPS high dosage (250 mg mL^{-1}). *p < 0.05 and **p < 0.01 (two-tailed t test); ns, not significant.

propria (LP) and epithelium of the mucosa where they defend potential pathogens by producing a specific immunoglobulin A (IgA) against their antigens. Therefore, they not only participate in local immunity but also play an essential role in the systemic immune response.[43] It has been demonstrated that plants polysaccharides can significantly regulate the immune activity of immune cells in PPs.[44,45] Cyclophosphamide is a commonly used chemotherapy drug. While killing cancer cells, it can inhibit the humoral and cellular immune responses, resulting in immunosuppression of body.[46] In this study, CTX was used to establish an immunosuppression mice model, resulting in an increase of T cells proportion in PPs and a decrease in the proportion of B cells, which is consistent with previous reports.[47] As we expected, PPPS eliminates the immunosuppressive state in PPs and enhances the stability of intestinal mucosal immunity. PPs cells are mainly composed of T/B cells. Moreover, T cells are known as a source of colony stimulating factor (CSFs) and various cytokines, which are involved in the proliferation response of multiple cells the bone marrow.[48] Our results have shown that T cells activated by PPPS contribute to the secretion of hematopoietic growth factors (*e.g.*, GM-CSF and IL-6) from PPs cells, participating in the systemic immune. Therefore, it could be assumed that PPPS modulates not only the mucosal immune system but also the systemic immune system PPs. Previous studies have demonstrated that PPPS was used as an immune adjuvant in oral vaccines to enhance the immune response.[49] Given the results in the present work, PPPS exhibits the immune-enhancing effect on the intestinal mucosal immune system, which may be associated with its ability to stimulate the immune activity of T and B lymphocytes in PPs. In addition, PPs also contain M cells, dendritic cells, macrophages, and other cells

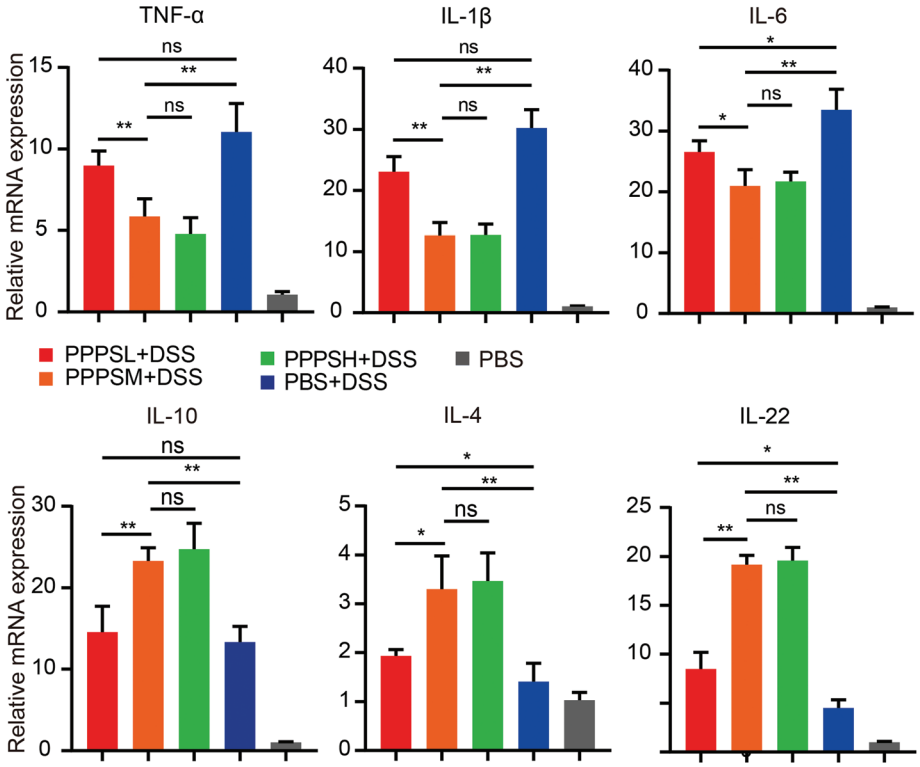

Fig. 6 PPPS can change the expression level of cytokines in colon tissue of mice with colitis. Relative mRNA expression of cytokine-related genes in colon tissue was examined by qPCR. The data are representative of three independent experiments (error bars, SD). PPPSL, PPPS low dosage (50 mg mL^{-1}); PPPSM, PPPS moderate dosage (125 mg mL^{-1}); PPPSH, PPPS high dosage (250 mg mL^{-1}). *$p < 0.05$ and **$p < 0.01$ (two-tailed t test); ns, not significant.

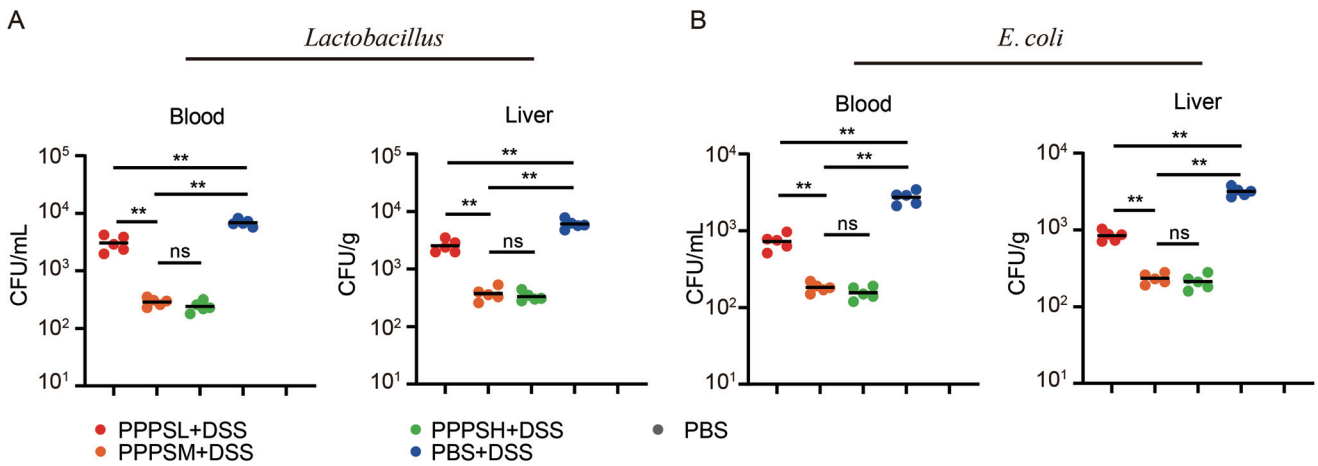

Fig. 7 PPPS can reduce the bacterial translocation in colitis. (A) The MRS plates was used to analysis *Lactobacillus* and the numbers of bacteria colonies in the blood and liver quantified as bacteria CFU. (B) The EMB plates was used to analysis *E. coli* the numbers of bacteria colonies in the blood and liver quantified as bacteria CFU. Each symbol represents an individual mouse. The data (A and B) are representative of three independent experiments (error bars, SD). PPPSL, PPPS low dosage (50 mg mL^{-1}); PPPSM, PPPS moderate dosage (125 mg mL^{-1}); PPPSH, PPPS high dosage (250 mg mL^{-1}). *$p < 0.05$ and **$p < 0.01$ (two-tailed t test); ns, not significant.

that are necessary for immune response.[50] In addition, when polysaccharides enter the posterior segment of the intestinal tract, they can be degraded by intestinal bacteria into small molecules, such as short-chain fatty acids, *etc.*, which will also affect the physiological functions of the intestinal tract.[51] However, whether PPPS or small molecules decomposed from PPPS played the leading role on regulating intestinal immunity needs to be further studied.

Epithelial cell homeostasis is essential for the physiological function of the intestinal barrier.[52] Tight junction (TJ) proteins, which are located at the top of the epithelium, connect the intestinal epithelial cells and respond to directional stimuli and transport functions.[53] The intestinal mucosal epithelial barrier plays a vital role in maintaining the stability of the internal environment and its integrity is required to prevent the occurrence and development of intestinal diseases.[54] So far, the epithelial cells are the strongest determinants of the physical intestinal barrier. ZO proteins are the scaffold-like TJ plaque proteins whose function is to anchor occludin and claudins to the cytoskeleton mesh network. Occludin and ZO-1 are required for typical TJ structure and development of barrier function. The decrease of its expression level or activities affects the integrity of the tightly connected structures between cells.[55] Lipopolysaccharide (LPS) is the main component of the cell wall of Gram negative bacteria, which can directly interact with intestinal mucosal epithelial cells to destroy the tight junction proteins, or indirectly interfere with the tight junction proteins, resulting in intestinal mucosal epithelial damage.[56] LPS contributes to the down-regulation and redistribution of TJ proteins in Caco2 monolayers, leading to an increase in epithelial permeability.[57] To date, little is known about the exact role of PPPS in regulating the function of epithelial barrier when exposed to LPS. In our present study, we have confirmed that PPPS-treated Caco2 cells can relieve the damage and maintain complete monolayer cell structure and function.

Colitis is a chronic inflammatory disease characterized by a continuous mucosal ulcer in the rectum and colon.[58] Oral administration of DSS to mice induces severe colitis, which is characterized by weight loss, bloody diarrhea, ulcer formation, loss of epithelial cells, and infiltrations with neutrophils. The induced mouse model accurately mimics human colitis.[59] The occurrence and development of UC caused by DSS are highly related to the imbalanced expression of inflammatory factors, including up-regulation of pro-inflammatory factors (*e.g.*, TNF-α, IL-1β, and IL-6) and down-regulation of anti-inflammatory factors (*e.g.*, IL-4 and IL-10).[60,61] The increasing inflammation in the colon will exacerbate the symptoms of colitis. In our study, the results have suggested that PPPS can relieve not only the clinical manifestations of colitis but also reduce the inflammatory responses in mice. It has been reported that IL-22 promotes epithelial cell proliferation and restores the dysregulated epithelial barrier function during DSS-induced colitis.[62] An increase of IL-22 in PPPS-treated colitis mice was also found, which indicates that PPPS can reduce intestinal damage. Intestinal bacteria can penetrate the intestinal mucosal barrier to invade healthy tissues and organs once the intestinal mucosal barrier is damaged, which may result in spontaneous peritonitis, bloodstream infection, and even systemic inflammatory response syndrome.[63] In this study, we have noticed that the two intestinal bacteria (*Lactobacillus* and *E. coli*) were significantly reduced in blood and liver of PPPS-treated mice, suggesting that the mice in the PPPS group had less colon damage. Besides, bacterial translocation can aggravate intestinal mucosal necrosis and bacterial translocation, resulting in a vicious circle. Current studies have shown that polysaccharides from a variety of plant sources, such as astragalus polysaccharides,[64,65] have preventive and protective effects on mouse colitis. Astragalus polysaccharides effectively relieve colitis in rats by restoring the functional status of T_{reg} cells and inhibiting the expression of IL-17 in PPs.[66] In this study, our results have only demonstrated that PPPS plays a role in the treatment of colitis by regulating the inflammatory response. However, further studies are still needed to assess if the efficacy is regulated by specific signaling pathways, which may be similar to Astragalus polysaccharides.

5. Conclusion

Our research has revealed that PPPS maintains intestinal balance, regulates the composition of gut microbiota, activates the lymphocytes in PPs, and protects the physical barrier of the intestinal epithelium. Furthermore, in the DSS-induced colitis mice model, PPPS can significantly alleviate the damage of colon. Overall, our results suggest that PPPS is a promising candidate for the development of a novel supplemental drug that promotes intestinal health.

Author contributions

RZ, DP, XN, and HS designed research. XN, HS, SC, RC, JH, YM, HWand WC performed research. XN, HS, ZS, DP, and RZ analyzed data. XN, HS, DP, and RZ wrote the paper.

Conflicts of interest

The authors declare that there is no conflict of interest.

Acknowledgements

This project was funded by the National Key Research and Development Program of China (2017YFD0500706). This project was supported by National Science Foundation of China (3177130834).

References

1 K. T. Fay, M. L. Ford and C. M. Coopersmith, The intestinal microenvironment in sepsis, *Biochim. Biophys. Acta, Mol. Basis Dis.*, 2017, **1863**, 2574–2583.
2 P. Hugenholtz and T. Huber, Chimeric 16S rDNA sequences of diverse origin are accumulating in the public databases, *Int. J. Syst. Evol. Microbiol.*, 2003, **53**, 289–293.
3 A. B. Shreiner, J. Y. Kao and V. B. Young, The gut microbiome in health and in disease, *Curr. Opin. Gastroenterol.*, 2015, **31**, 69–75.

4 M. G. Rooks and W. S. Garrett, Gut microbiota, metabolites and host immunity, *Nat. Rev. Immunol.*, 2016, **16**, 341–352.
5 B. Ahluwalia, M. K. Magnusson and L. Ohman, Mucosal immune system of the gastrointestinal tract: maintaining balance between the good and the bad, *Scand. J. Gastroenterol.*, 2017, **52**, 1185–1193.
6 N. J. Mantis, N. Rol and B. Corthesy, Secretory IgA's complex roles in immunity and mucosal homeostasis in the gut, *Mucosal Immunol.*, 2011, **4**, 603–611.
7 A. T. Blikslager, A. J. Moeser, J. L. Gookin, S. L. Jones and J. Odle, Restoration of barrier function in injured intestinal mucosa, *Physiol. Rev.*, 2007, **87**, 545–564.
8 S. Broer, Amino acid transport across mammalian intestinal and renal epithelia, *Physiol. Rev.*, 2008, **88**, 249–286.
9 M. Saleh and G. Trinchieri, Innate immune mechanisms of colitis and colitis-associated colorectal cancer, *Nat. Rev. Immunol.*, 2011, **11**, 9–20.
10 I. Loddo and C. Romano, Inflammatory Bowel Disease: Genetics, Epigenetics, and Pathogenesis, *Front. Immunol.*, 2015, **6**, 551.
11 A. R. Saniabadi, T. Tanaka, T. Ohmori, K. Sawada, T. Yamamoto and H. Hanai, Treating inflammatory bowel disease by adsorptive leucocytapheresis: a desire to treat without drugs, *World J. Gastroenterol.*, 2014, **20**, 9699–9715.
12 C. Delattre, T. A. Fenoradosoa and P. Michaud, Galactans: an overview of their most important sourcing and applications as natural polysaccharides, *Braz. Arch. Biol. Technol.*, 2011, **54**, 1075–1092.
13 M. Yin, Y. Zhang and H. Li, Advances in Research on Immunoregulation of Macrophages by Plant Polysaccharides, *Front. Immunol.*, 2019, **10**, 145.
14 R. Jiao, Y. Liu, H. Gao, J. Xiao and K. F. So, The Anti-Oxidant and Antitumor Properties of Plant Polysaccharides, *Am. J. Chin. Med.*, 2016, **44**, 463–488.
15 J. Tian, X. Hu, D. Liu, H. Wu and L. Qu, Identification of Inonotus obliquus polysaccharide with broad-spectrum antiviral activity against multi-feline viruses, *Int. J. Biol. Macromol.*, 2017, **95**, 160–167.
16 L. Xu, F. Yang, J. Wang, H. Huang and Y. Huang, Anti-diabetic effect mediated by Ramulus mori polysaccharides, *Carbohydr. Polym.*, 2015, **117**, 63–69.
17 J. H. Xie, M. L. Jin, G. A. Morris, X. Q. Zha, H. Q. Chen, Y. Yi, J. E. Li, Z. J. Wang, J. Gao, S. P. Nie, P. Shang and M. Y. Xie, Advances on Bioactive Polysaccharides from Medicinal Plants, *Crit. Rev. Food Sci. Nutr.*, 2016, **56**(Suppl 1), S60–S84.
18 S. Yang, K. Wei, F. Jia, X. Zhao, G. Cui, F. Guo and R. Zhu, Characterization and biological activity of Taishan Pinus massoniana pollen polysaccharide in vitro, *PLoS One*, 2015, **10**, e0115638.
19 C. Pastori and L. Lopalco, Isolation and in vitro Activation of Mouse Peyer's Patch Cells from Small Intestine Tissue, *Bio-Protoc.*, 2014, **4**, e1282.
20 K. W. Yu, H. Kiyohara, T. Matsumoto, H. C. Yang and H. Yamada, Intestinal immune system modulating polysaccharides from rhizomes of Atractylodes lancea, *Planta Med.*, 1998, **64**, 714–719.
21 S. Wirtz, C. Neufert, B. Weigmann and M. F. Neurath, Chemically induced mouse models of intestinal inflammation, *Nat. Protoc.*, 2007, **2**, 541–546.
22 C. He, Y. Shi, R. Wu, M. Sun, L. Fang, W. Wu, C. Liu, M. Tang, Z. Li, P. Wang, Y. Cong and Z. Liu, miR-301a promotes intestinal mucosal inflammation through induction of IL-17A and TNF-alpha in IBD, *Gut*, 2016, **65**, 1938–1950.
23 B. Li, K. Wei, S. Yang, Y. Yang, Y. Zhang, F. Zhu, D. Wang and R. Zhu, Immunomodulatory effects of Taishan Pinus massoniana pollen polysaccharide and propolis on immunosuppressed chickens, *Microb. Pathog.*, 2015, **78**, 7–13.
24 C. Yu, K. Wei, L. Liu, S. Yang, L. Hu, P. Zhao, X. Meng, M. Shao, C. Wang, L. Zhu, H. Zhang, Y. Li and R. Zhu, Taishan Pinus massoniana pollen polysaccharide inhibits subgroup J avian leucosis virus infection by directly blocking virus infection and improving immunity, *Sci. Rep.*, 2017, **7**, 44353.
25 X. Zhao, M. Liang, P. Yang, F. Guo, D. Pan, X. Huang, Y. Li, C. Wu, T. Qu and R. Zhu, Taishan Pinus massoniana pollen polysaccharides promote immune responses of recombinant Bordetella avium ompA in BALB/c mice, *Int. Immunopharmacol.*, 2013, **17**, 793–798.
26 J. Lachar and J. S. Bajaj, Changes in the Microbiome in Cirrhosis and Relationship to Complications: Hepatic Encephalopathy, Spontaneous Bacterial Peritonitis, and Sepsis, *Semin. Liver Dis.*, 2016, **36**, 327–330.
27 N. Wang, Q. Han, G. Wang, W. P. Ma, J. Wang, W. X. Wu, Y. Guo, L. Liu, X. Y. Jiang, X. L. Xie and H. Q. Jiang, Resveratrol Protects Oxidative Stress-Induced Intestinal Epithelial Barrier Dysfunction by Upregulating Heme Oxygenase-1 Expression, *Dig. Dis Sci.*, 2016, **61**, 2522–2534.
28 J. Sun and E. B. Chang, Exploring gut microbes in human health and disease: Pushing the envelope, *Genes Dis.*, 2014, **1**, 132–139.
29 I. Lagkouvardos, T. R. Lesker, T. C. A. Hitch, E. J. C. Galvez, N. Smit, K. Neuhaus, J. Wang, J. F. Baines, B. Abt, B. Stecher, J. Overmann, T. Strowig and T. Clavel, Sequence and cultivation study of Muribaculaceae reveals novel species, host preference, and functional potential of this yet undescribed family, *Microbiome*, 2019, **7**, 28.
30 T. S. Stappenbeck, L. V. Hooper and J. I. Gordon, Developmental regulation of intestinal angiogenesis by indigenous microbes via Paneth cells, *Proc. Natl. Acad. Sci. U. S. A.*, 2002, **99**, 15451–15455.
31 C. L. Sears, A dynamic partnership: celebrating our gut flora, *Anaerobe*, 2005, **11**, 247–251.
32 G. D. Wu, J. Chen, C. Hoffmann, K. Bittinger, Y. Y. Chen, S. A. Keilbaugh, M. Bewtra, D. Knights, W. A. Walters, R. Knight, R. Sinha, E. Gilroy, K. Gupta, R. Baldassano, L. Nessel, H. Li, F. D. Bushman and J. D. Lewis, Linking long-term dietary patterns with gut microbial enterotypes, *Science*, 2011, **334**, 105–108.
33 J. G. LeBlanc, C. Milani, G. S. de Giori, F. Sesma, D. van Sinderen and M. Ventura, Bacteria as vitamin suppliers to

their host: a gut microbiota perspective, *Curr. Opin. Biotechnol*, 2013, **24**, 160–168.

34 R. Toure, E. Kheadr, C. Lacroix, O. Moroni and I. Fliss, Production of antibacterial substances by bifidobacterial isolates from infant stool active against Listeria monocytogenes, *J. Appl. Microbiol.*, 2003, **95**, 1058–1069.

35 Y. X. Yang, M. He, G. Hu, J. Wei, P. Pages, X. H. Yang and S. Bourdu-Naturel, Effect of a fermented milk containing Bifidobacterium lactis DN-173010 on Chinese constipated women, *World J. Gastroenterol.*, 2008, **14**, 6237–6243.

36 H. S. Ejtahed, J. Mohtadi-Nia, A. Homayouni-Rad, M. Niafar, M. Asghari-Jafarabadi and V. Mofid, Probiotic yogurt improves antioxidant status in type 2 diabetic patients, *Nutrition*, 2012, **28**, 539–543.

37 J. Z. Xiao, S. Kondo, N. Takahashi, K. Miyaji, K. Oshida, A. Hiramatsu, K. Iwatsuki, S. Kokubo and A. Hosono, Effects of Milk Products Fermented by Bifidobacterium longum on Blood Lipids in Rats, and Healthy Adult Male Volunteers, *J. Dairy Sci.*, 2003, **86**(0022-0302), 2452–2461.

38 O. T. Burton, A. R. Darling, J. S. Zhou, M. Noval-Rivas, T. G. Jones, M. F. Gurish, T. A. Chatila and H. C. Oettgen, Direct effects of IL-4 on mast cells drive their intestinal expansion and increase susceptibility to anaphylaxis in a murine model of food allergy, *Mucosal Immunol.*, 2013, **6**, 740–750.

39 L. Han, H. Jin, L. Zhou, X. Zhang, Z. Fan, M. Dai, Q. Lin, F. Huang, L. Xuan, H. Zhang and Q. Liu, Intestinal Microbiota at Engraftment Influence Acute Graft-Versus-Host Disease via the Treg/Th17 Balance in Allo-HSCT Recipients, *Front. Immunol.*, 2018, **9**, 669.

40 L. Zhao, W. Windisch and M. Kirchgessner, A study on the nutritive value of pollen from the Chinese Masson Pine (Pinus massoniana) and its effect on fecal characteristics in rats, *Z. Ernahrungswiss.*, 1996, **35**, 341–347.

41 C. Wagner, J. Bonnardel, C. Da Silva, L. Martens, J. P. Gorvel and H. Lelouard, Some news from the unknown soldier, the Peyer's patch macrophage, *Cell. Immunol.*, 2018, **330**, 159–167.

42 S. C. Corr, C. C. G. M. Gahan and C. Hill, M-cells: origin, morphology and role in mucosal immunity and microbial pathogenesis, *FEMS Immunol. Med. Microbiol.*, 2008, **52**, 2–12.

43 K. Fujihashi, T. Dohi, P. D. Rennert, M. Yamamoto, T. Koga, H. Kiyono and J. R. McGhee, Peyer's patches are required for oral tolerance to proteins, *Proc. Natl. Acad. Sci. U. S. A.*, 2001, **98**, 3310–3315.

44 H. J. Suh, H. S. Yang, K. S. Ra, D. O. Noh, K. H. Kwon, J. H. Hwang and K. W. Yu, Peyer's patch-mediated intestinal immune system modulating activity of pectic-type polysaccharide from peel of Citrus unshiu, *Food Chem.*, 2013, **138**, 1079–1086.

45 Y. N. Georgiev, B. S. Paulsen, H. Kiyohara, M. Ciz, M. H. Ognyanov, O. Vasicek, F. Rise, P. N. Denev, H. Yamada, A. Lojek, V. Kussovski, H. Barsett, A. I. Krastanov, I. Z. Yanakieva and M. G. Kratchanova, The common lavender (Lavandula angustifolia Mill.) pectic polysaccharides modulate phagocytic leukocytes and intestinal Peyer's patch cells, *Carbohydr. Polym.*, 2017, **174**, 948–959.

46 R. Wojcik, Reactivity of the immunological system of rats stimulated with Biolex-Beta HP after cyclophosphamide immunosuppression, *Cent. Eur. J. Immunol.*, 2014, **39**, 51–60.

47 C. F. Kuper, M. Van Zijverden, C. Klaassen, M. Tegelenbosch-Schouten and A. P. Wolterbeek, Effects of cyclosporin A and cyclophosphamide on Peyer's patches in rat, exposed in utero and neonatally or during adult age, *Toxicol. Pathol.*, 2007, **35**, 226–232.

48 Y. Shi, C. H. Liu, A. I. Roberts, J. Das, G. Xu, G. Ren, Y. Zhang, L. Zhang, Z. R. Yuan, H. S. Tan, G. Das and S. Devadas, Granulocyte-macrophage colony-stimulating factor (GM-CSF) and T-cell responses: what we do and don't know, *Cell Res.*, 2006, **16**, 126–133.

49 J. Zhou, K. Wei, C. Wang, W. Dong, N. Ma, L. Zhu, L. P. Hu, H. Huang and R. Zhu, Oral immunisation with Taishan Pinus massoniana pollen polysaccharide adjuvant with recombinant Lactococcus lactis-expressing Proteus mirabilis ompA confers optimal protection in mice, *Allergol. Immunopathol.*, 2017, **45**, 496–505.

50 M. Ebisawa, K. Hase, D. Takahashi, H. Kitamura, K. A. Knoop, I. R. Williams and H. Ohno, CCR6hiCD11c (int) B cells promote M-cell differentiation in Peyer's patch, *Int. Immunol.*, 2011, **23**, 261–269.

51 H. Yoshikawa, K. Takada and S. Muranishi, Molecular weight-dependent lymphatic transfer of exogenous macromolecules from large intestine of renal insufficiency rats, *Pharm. Res.*, 1992, **9**, 1195–1198.

52 X. Wang, M. C. Valenzano, J. M. Mercado, E. P. Zurbach and J. M. Mullin, Zinc supplementation modifies tight junctions and alters barrier function of CACO-2 human intestinal epithelial layers, *Dig. Dis Sci.*, 2013, **58**, 77–87.

53 J. Konig, J. Wells, P. D. Cani, C. L. Garcia-Rodenas, T. MacDonald, A. Mercenier, J. Whyte, F. Troost and R. J. Brummer, Human Intestinal Barrier Function in Health and Disease, *Clin. Transl. Gastroenterol.*, 2016, **7**, e196.

54 L. Shen, L. Su and J. R. Turner, Mechanisms and functional implications of intestinal barrier defects, *Dig. Dis.*, 2009, **27**, 443–449.

55 A. Betanzos, R. Javier-Reyna, G. Garcia-Rivera, C. Banuelos, L. Gonzalez-Mariscal, M. Schnoor and E. Orozco, The EhCPADH112 complex of Entamoeba histolytica interacts with tight junction proteins occludin and claudin-1 to produce epithelial damage, *PLoS One*, 2013, **8**, e65100.

56 X. Han, M. P. Fink, R. Yang and R. L. Delude, Increased iNOS activity is essential for intestinal epithelial tight junction dysfunction in endotoxemic mice, *Shock*, 2004, **21**, 261–270.

57 S. Lei, T. Cheng, Y. Guo, C. Li, W. Zhang and F. Zhi, Somatostatin ameliorates lipopolysaccharide-induced tight junction damage via the ERK-MAPK pathway in Caco2 cells, *Eur. J. Cell Biol.*, 2014, **93**, 299–307.

58 M. D. Kappelman, S. L. Rifas-Shiman, K. Kleinman, D. Ollendorf, A. Bousvaros, R. J. Grand and J. A. Finkelstein, The prevalence and geographic distribution of Crohn's disease and ulcerative colitis in the United States, *Clin. Gastroenterol. Hepatol.*, 2007, **5**, 1424–1429.

59 I. Okayasu, S. Hatakeyama, M. Yamada, T. Ohkusa, Y. Inagaki and R. Nakaya, A novel method in the induction of reliable experimental acute and chronic ulcerative colitis in mice, *Gastroenterology*, 1990, **98**, 694–702.

60 Z. Zhang, L. Yang, B. Wang, L. Zhang, Q. Zhang, D. Li, S. Zhang, H. Gao and X. Wang, Protective role of liriodendrin in mice with dextran sulphate sodium-induced ulcerative colitis, *Int. Immunopharmacol.*, 2017, **52**, 203–210.

61 Y. H. Li, R. Adam, J. F. Colombel and Z. X. Bian, A characterization of pro-inflammatory cytokines in dextran sulfate sodium-induced chronic relapsing colitis mice model, *Int. Immunopharmacol.*, 2018, **60**, 194–201.

62 J. L. Bishop, M. E. Roberts, J. L. Beer, M. Huang, M. K. Chehal, X. Fan, L. A. Fouser, H. L. Ma, J. T. Bacani and K. W. Harder, Lyn activity protects mice from DSS colitis and regulates the production of IL-22 from innate lymphoid cells, *Mucosal Immunol.*, 2014, **7**, 405–416.

63 J. MacFie, C. O'Boyle, C. J. Mitchell, P. M. Buckley, D. Johnstone and P. Sudworth, Gut origin of sepsis: a prospective study investigating associations between bacterial translocation, gastric microflora, and septic morbidity, *Gut*, 1999, **45**, 223–228.

64 J. Lv, Y. Zhang, Z. Tian, F. Liu, Y. Shi, Y. Liu and P. Xia, Astragalus polysaccharides protect against dextran sulfate sodium-induced colitis by inhibiting NF-kappacapital VE, Cyrillic activation, *Int. J. Biol. Macromol.*, 2017, **98**, 723–729.

65 M. Yang, H.-B. Lin, S. Gong, P.-Y. Chen, L.-L. Geng, Y.-M. Zeng and D.-Y. Li, Effect of Astragalus polysaccharides on expression of TNF-α, IL-1β and NFATc4 in a rat model of experimental colitis, *Cytokine*, 2014, **70**, 81–86.

66 H. M. Zhao, Y. Wang, X. Y. Huang, M. F. Huang, R. Xu, H. Y. Yue, B. G. Zhou, H. Y. Huang, Q. M. Sun and D. Y. Liu, Astragalus polysaccharide attenuates rat experimental colitis by inducing regulatory T cells in intestinal Peyer's patches, *World J. Gastroenterol.*, 2016, **22**, 3175–3185.

